Variable-Temperature ^{17}O NMR Study of Oxygen Motion in the Anionic Conductor $Bi_{26}Mo_{10}O_{69}$

Lesley Holmes,[†] Luming Peng,[†] Ivo Heinmaa,[‡] Luke A. O'Dell,[§] Mark E. Smith,[§] Rose-Noelle Vannier,[||] and Clare P. Grey*,[†]

Department of Chemistry, State University of New York at Stony Brook, Stony Brook, New York 11794−3400, National Institute of Chemical Physics and Biophysics, 12618 Tallinn, Estonia, Department of Physics, University of Warwick, Coventry, CV4 7AL United Kingodm, and Unité de Catalyse et Chimie du Solide, Equipe de Chimie du Solide, ENSCL/Université des Sciences et Technologies de Lille 1, BP 90 108, 59652 Villeneuve d'Ascq Cedex, France

Received February 3, 2008. Revised Manuscript Received April 4, 2008

Variable-temperature ^{17}O NMR spectroscopy, spanning a temperature range from −238 to 1000 °C, has been used to investigate mechanisms for ionic conduction in $Bi_{26}Mo_{10}O_{69}$, a material that contains both MoO_4^{2-} tetrahedra and $[Bi_{12}O_{14}]^{8-}{}_\infty$ columns. Two ^{17}O NMR resonances are observed that are assigned to oxygen atoms in the MoO_4^{2-} tetrahedra and in the $[Bi_{12}O_{14}]^{8-}{}_\infty$ columns. On the basis of the nutation curves for the two groups of resonances, extremely rapid, but local, reorientational motion of the MoO_4^{2-} units occurs at −70 °C and above (with a frequency of >50 kHz), whereas the Bi−O oxygen ions are rigid in this temperature regime. This is confirmed by both an analysis of the line broadening of the ^{17}O MoO_4^{2-} satellite transitions (under MAS) and the spin−lattice relaxation (T_1) times of these sites, the T_1 times indicating that the MoO_4^{2-} reorientation rates rapidly increase, reaching >100 MHz at 400 °C. Line narrowing of the MoO_4^{2-} central-transition resonance indicates that exchange between the tetrahedral units, a motion required for long-range anionic conduction, is much slower, involving only jump rates of approximately 1 kHz at 200 °C. Both the changes in line width of the MoO_4^{2-} resonance, and the jump in the T_1 times of the oxygen atoms in the $[Bi_{12}O_{14}]^{8-}{}_\infty$ columns at around the triclinic-monoclinic phase transition temperature (310 °C) are consistent with a mechanism for motion involving all the oxygen atoms. The predicted conductivity based on the [Bi−O] T_1 times is now of the order of that extracted from ac impedance measurements reported by Vannier et al. (*J. Solid State Chem.* **1996**, *122*, 394). On the basis of this detailed NMR analysis, we propose that motion at ambient temperatures primarily involves the MoO_4^{2-} tetrahedral rotation: exchange between these sites is very slow. At higher temperatures (above 310 °C), the conduction process now appears to involve the oxygen atoms coordinated to Bi^{3+}, in the $[Bi_{12}O_{14}]^{8-}{}_\infty$ columns, and most likely in the partially vacant O[19] site. The involvement of these sites allows for long-range conduction processes that do not involve concerted, multiple Mo−O bond breakages.

Introduction

Anionic conductors are used in a growing number of applications including oxygen sensors in catalytic converters, membranes for oxygen/nitrogen separation, and as electrolytes in solid oxide fuel cells, all of these applications requiring high O^{2-} transport. For the materials currently in use, conduction is very limited except at high temperatures (>800 °C). Even the widely employed yttrium stabilized zirconia (YSZ) exhibits rapid oxygen-ion motion only at temperatures above 700 °C. Due to the practical difficulties and costs associated with the use of materials that can operate at these temperatures, it is important to identify electrolytes with higher levels of anionic conduction at lower temperatures and to understand the structural factors that promote this high conductivity. Currently, bismuth-rich molybdates and vanadates (Bi/Mo(V) ≥ 2) have been shown to exhibit high oxide ion conductivity. Of these materials, the doped bismuth vanadium oxides (the so-called BiMeVOx's Me = Cu, Co) have the highest oxide ion conductivity of any material yet reported.[1] The structures of the BiMeVOx's (and the related molybate Bi_2MoO_6) consist of defect Aurivillius phases composed of perovskite-like sheets comprising corner-sharing $VO_{6-\delta}^{(7-2\delta)-}$ (or MoO_6^{6-}) polyhedra alternating with $Bi_2O_2^{2+}$ layers. The motion predominantly occurs in the perovskite-derived sheets. Molybdates with an even higher Bi^{3+} content (solid solutions around the composition Bi/Mo ∼ 2.6) adopt a very different structure, which contains MoO_4^{2-} anions, and yet also show good anionic conductivity.[2–6] The purpose of the research described in this paper is to

* Corresponding author. E-mail: cgrey@notes.cc.sunysb.edu.
[†] State University of New York at Stony Brook.
[‡] National Institute of Chemical Physics and Biophysics.
[§] University of Warwick.
[||] Université des Sciences et Technologies de Lille 1.

(1) Abraham, F.; Boivin, J. C.; Mairesse, G.; Nowogrocki, G. *Solid State Ionics* **1990**, *934*, 40–41.
(2) Vannier, R.-N.; Mairesse, G.; Abraham, F.; Nowogrocki, G. *J. Solid State Chem.* **1996**, *122*, 394.
(3) Vannier, R.-N.; Danzé, S.; Nowogrocki, G.; Huvé, M.; Mairesse, G. *Solid State Ionics* **2000**, *51*, 136–137.
(4) Vannier, R.-N.; Abraham, F.; Nowogrocki, G.; Mairesse, G. *J. Solid State Chem.* **1999**, *142*, 294.
(5) Galy, J.; Salles, P.; Rozier, P.; Castro, A. *Solid State Ionics* **2006**, *177*, 6.

10.1021/cm800351c CCC: $40.75
Published on Web 05/14/2008

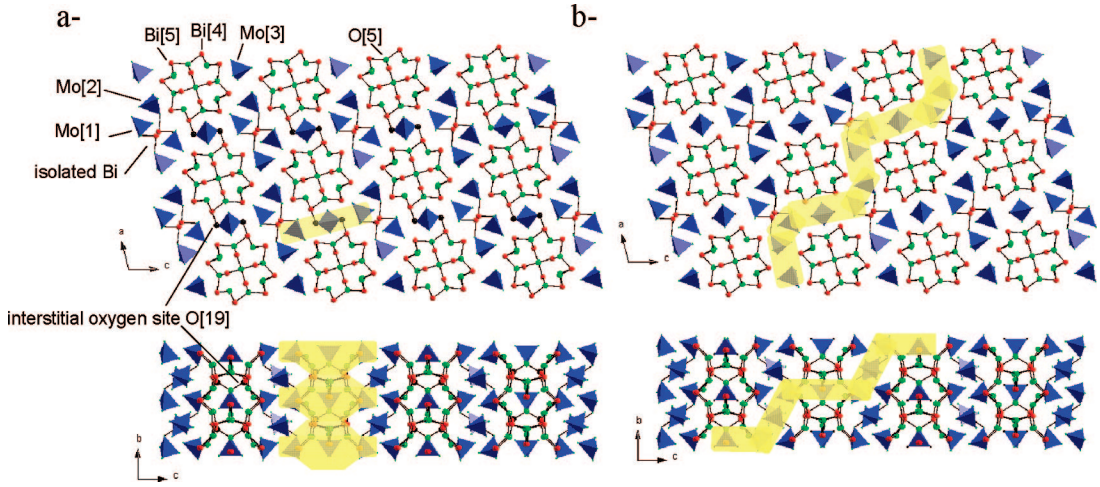

Figure 1. Structure of $Bi_{26}Mo_{10}O_{69}$ showing, in yellow, the preferential oxygen pathways proposed by (a) Vannier et al.[3] and (b) Galy et al.[5] in the *a*, *c* and *b*, *c* planes. Red spheres represent bismuth, green spheres represent oxygen, and blue tetrahedra represent MoO_4^{2-} units. The O(19) interstitial sites proposed by Vannier are indicated. Coordinates were taken from ref 3; bond lengths up to 2.36 Å were used for the Bi−O connectivity.

investigate the nature of the local motion in the bismuth-rich material $Bi_{26}Mo_{10}O_{69}$, by using ^{17}O MAS NMR spectroscopy and to combine these results with longer probes of motion such as ac susceptibility.

The parent composition, $Bi_{26}Mo_{10}O_{69}$, is a pure oxide ion conductor (i.e., there is a negligible electronic contribution) with a conductivity of 1 mS/cm at 500 °C and a low activation energy of only 0.47 eV. On cooling, it undergoes a phase transition at 310 °C from a monoclinic to a triclinic structure, which is characterized by a decrease of the conductivity and a noticeable increase of the activation energy to 1.05 eV.[2] A solubility range of $2.57 \leq Bi/Mo \leq 2.77$ was determined for these materials by Vannier et al.[2] and confirmed by Buttrey et al.[7] In contrast, Galy and co-workers, in their more recent work, reported a larger solid solution domain of $2.53 < Bi/Mo \leq 3.50$,[8] which was larger than the values that they had originally proposed.[6] The skeleton of the structure is composed of MoO_4^{2-} tetrahedra interspersed with $[Bi_{12}O_{14}]_\infty$ columns and an isolated bismuth ion (Figure 1). The structure of $Bi_{26}Mo_{10}O_{69}$ at room temperature was refined in the *P*2/*c* space group by Vannier[2] and Buttrey.[7] The small triclinic distortion could not be taken into account in these refinements. Both groups observed full occupancy of the isolated bismuth site and suggested that an interstitial oxygen site must be present to ensure overall charge balance (with the Bi^{3+} and Mo^{6+} ions). This model was in good agreement with the density measurements (7.54 g/cm^3 compared to a calculated value of 7.53 g/cm^3).[2] Large anisotropic displacement parameters for the oxygen atoms in the MoO_4^{2-} tetrahedra were observed when compared to those in $[Bi_{12}O_{14}]_\infty$ columns, suggesting that oxygen motion in $Bi_{26}Mo_{10}O_{69}$ occurs within the Mo units. In their model, Buttery et al. located the extra oxygen site close to the isolated bismuth atom but obtained short O−O distances of 2.1 Å. They also showed that the structure could be viewed as the intergrowth of fluorite-like bands and a "monoclinic variation of the cation arrangement". These monoclinic regions are very similar to the fluorite lattice and by comparing the structural model of "$Bi_{26}Mo_{10}O_{68}$" with the fluorite structure, Vannier et al. found a 4g empty site at ∼0.45, ∼0.40, ∼0.15, which they labeled O(19).[3] This O(19) interstitial site is coordinated to two Bi^{3+} atoms (Bi(4) and Bi(5)) and is located between two $Mo(3)O_4$ tetrahedra as shown in Figure 1a. Because of the short distances (2.5−2.9 Å) between oxygen atoms belonging to $Mo(1)O_4$ and $Mo(3)O_4$ tetrahedra and this interstitial site, an oxygen diffusion pathway along the [0 1 0] direction was proposed by these authors involving these tetrahedra and the O[19] site, as shown in yellow in Figure 1a. Because of the relatively long O−O distances between O atoms of the $Mo(1)O_4^{2-}$ and $Mo(2)O_4^{2-}$ tetrahedra, long-range conductivity involving the $Mo(1)O_4^{2-}$ tetrahedra, (i.e., in the *a*−*c* plane) was excluded. The materials were therefore proposed to be monodimensional oxide ion conductors, with conduction occurring along the directions of the columns (the *b*-direction). In contrast, Galy et al. proposed the following general formula to explain the solid solution extension, $Bi_{(2+x)/3}\square_{(1-x)/3}[Bi_{12}O_{14}][MoO_4]_{5-x}[BiO_3]_x$ with $0 \leq x \leq 1$, and viewed the structure as being built from MoO_4^{2-} and $BiEO_3$ tetrahedra (E being the bismuth cation lone pair) in $[Bi_{12}O_{14}]_\infty$ columns and an isolated bismuth ion.[8] The composition Bi/Mo = 2.6 then corresponds to two $Bi_{0.695}\square_{0.305}[Bi_{12}O_{14}][MoO_4]_{4.913}[BiO_3]_{0.087}$ units per cell. Note that this leads to a theoretical density of 7.40 kg/m^3 instead of 7.54 kg/m^3 measured by Vannier et al. The oxygen diffusion was suggested to occur via a cooperative mechanism along the [2 0 1] direction, in which all the MoO_4^{2-} tetrahedra are involved, but no oxygen vacancies or interstitial sites (Figure 1b).

The prior work on these systems highlights the complexity of both the structures of these materials and the conduction mechanisms. The mechanisms for conduction in this material remain controversial[2−6] and it is clear that further measurements are required to test the different models for conduction. While impedance studies have yielded the values for the

(6) Enjalbert, R.; Hasselmann, G.; Galy, J. *J. Solid State Chem.* **1997**, *131*, 236.
(7) Buttery, D. J.; Vogt, T.; Yap, G. P. A.; Rheingold, A. L. *Mater. Res. Bull.* **1997**, *32*, 947.
(8) Galy, J.; Enjalbert, R.; Rozier, P.; Millet, P. *Solid State Sci.* **2003**, *5*, 165.

long-range ionic motion, they can not be used to determine the pathway(s) or the local dynamics responsible for the conduction, nor do they provide information concerning which type of oxygen site is responsible for the motion. Also, while insight into the possible mobile species can be extracted from diffraction studies, the technique does not provide a direct measure of the exchange rates between different oxygen sublattices. To provide such information, ^{17}O NMR methods have been successfully applied to a wide range of ionic conductors.[9,10] For example, in our previous work[9] on the Aurivillius phase Bi_2WO_6, three resonances could be identified in the one-dimensional magic angle spinning (MAS) NMR spectrum, which were assigned to oxygens coordinated solely to bismuth (O−Bi_4), tungsten (W−O−W), or bridging between both bismuth and tungsten (Bi−O−W) ions. Once the different species were identified, it was then possible to discern the different conduction pathways associated with these ions: Oxygen mobility in the tungstate layers was identified by variable temperature 1D MAS NMR, while slower exchange rates between the tungstate and bismuth layers was identified by two-dimensional (2D) magnetization exchange methods. Thus, the objective of the work presented here is to use ^{17}O NMR methods to determine the conduction mechanism and to establish how the unique structure of bismuth molybdate controls the movement of oxygen atoms in this compound. We apply a wide range of NMR spectroscopic techniques to investigate motion in $Bi_{26}Mo_{10}O_{69}$, because the hopping rates were found to span more than 5 orders of magnitude over the temperature range investigated. 2D magnetization exchange methods were not feasible due to very short spin−lattice relaxation times observed for this material. The results are combined with prior ac impedance measurements,[2] which probe longer range motion. We show that while the molybdate units are rotating extremely rapidly (with rates of ∼2 MHz), even at room temperature, conductivity also involves exchange with the oxygen atoms coordinated to Bi^{3+} ions.

Experimental Section

Preparation, diffraction studies and ac impedance measurements of $Bi_{26}Mo_{10}O_{69}$ powder were described previously by Vannier et al.[2] ^{17}O enrichment was performed by heating a quartz tube containing a small quantity of the sample to 500 °C in a $^{17}O_2$ environment (Isotec min. 50 at %) for 24 h.

Room- and high-temperature MAS NMR experiments were carried out at SUNY Stony Brook at 67.78 MHz (11.7 T) on a Varian InfinityPlus-500 spectrometer equipped with a Chemagnetics 4 mm HXY probe with pulse widths of 1.5 μs a pulse delay of 1 s, at a spinning speed of 15 kHz, and using approximately 30 000 scans. Ultra low and high temperature experiments were carried out at the National Institute of Chemical Physics and Biophysics in Tallinn, Estonia, where low-temperature MAS experiments were carried out at 48.8 MHz (8.45 T) on a Bruker AMX360 spectrometer with a Cryo-MAS™ 1.8 mm probe[11] built by the Samoson group,[11,12] with pulse widths of 1.2 μs, a pulse delay of 2 s, at a spinning speed of 25 kHz using helium for bearing, drive, and temperature control, and using approximately 200 scans. High-temperature static experiments were carried out at 48.8 MHz on a Bruker AMX360 spectrometer with a home-built 5 mm HX probe using pulse widths of 3.5 μs, a pulse delay of 0.1 s, and approximately 5600 scans. Ultra high temperature experiments were carried out at the University of Warwick in Coventry, United Kingdom, at 81.3 MHz (14.1 T) on a Bruker Avance II$^+$ 600 spectrometer equipped with a home-built 7.5 mm single channel probe[13] using a pulse width of 15 μs, a pulse delay of 0.1 s and approximately 7400 scans. Experiments were performed with a rotor synchronized Hahn-echo pulse sequence ($\pi/6 - \tau - \pi/3 - \tau$) to avoid probe ringing. A one-pulse experiment was used for the ultra high temperature experiments, due to the poor signal-to-noise (S/N) at these temperatures. Nutation and T_1 experiments were performed by varying the pulse length and pulse delay, respectively.

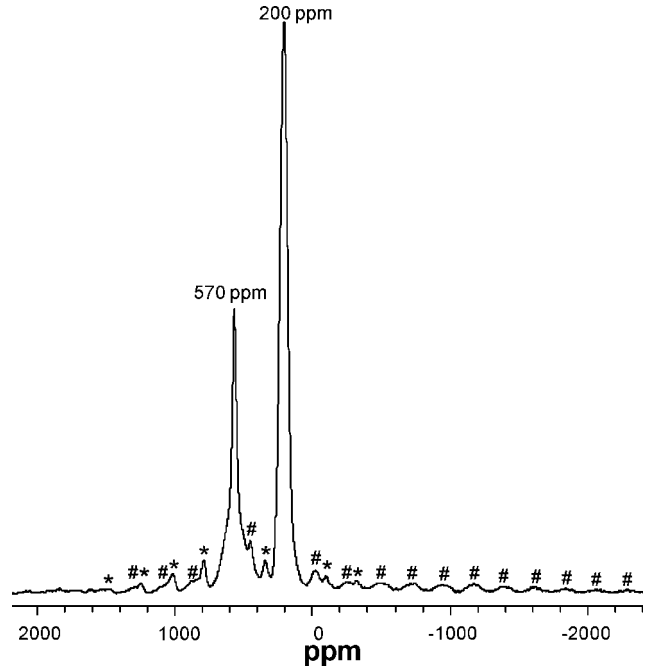

Figure 2. ^{17}O MAS NMR echo spectrum of $Bi_{26}Mo_{10}O_{69}$ acquired with short ($\pi/6$, $\pi/3$) pulse widths and a pulse delay of 1 s at a spinning speed of 15 kHz at 67.7 MHz. Chemical shifts of the isotropic resonances are indicated in this and subsequent spectra. Sidebands from the 570 and 200 ppm resonances are marked with "*" and "#", respectively. The broad resonances, seen clearly between −200 and −2000 ppm, are the satellite transitions from the 200 ppm resonance. (N.b., satellite transitions are also seen at high frequencies; these, however, are much weaker because of the characteristics of the probe, which has an asymmetric tuning "dip").

Results

Room- and Low-Temperature MAS NMR. The ^{17}O MAS NMR spectrum of $Bi_{26}Mo_{10}O_{69}$ is shown in Figure 2. Although there are 19 different O crystallographic sites in this compound, only two distinct resonances are observed at 200 and 570 ppm. The resonance at 200 ppm is assigned to oxygen atoms coordinated to bismuth ions based on previous ^{17}O NMR studies by Yang et al.[14] of Bi_2O_3 (195 ppm), and on our work on the BiMeVOx[10] systems and

(9) Kim, N.; Vannier, R.-N.; Grey, C. P. *Chem. Mater.* **2005**, *17*, 1952.
(10) Kim, N.; Grey, C. P. *Science* **2002**, *297*, 1317.
(11) Samoson, A.; Tuherm, T.; Past, J.; Reinhold, A.; Anupold, T.; Heinmaa, I. *Top. Curr. Chem.* **2005**, *246*, 15.
(12) Samoson, A.; Heinmaa, I.; Tuherm, T.; Reinhold, A.; Past, J.; Stern, R.; Anupold, T. Patent WO/2005/101949, 2005.
(13) O'Dell, L. A.; Savin, S. L. P.; Chadwick, A. V.; Smith, M. E. *Faraday Discuss.* **2007**, *134*, 83.
(14) Yang, S.; Park, K. D.; Oldfield, E. *J. Am. Chem. Soc.* **1989**, *111*, 7278.

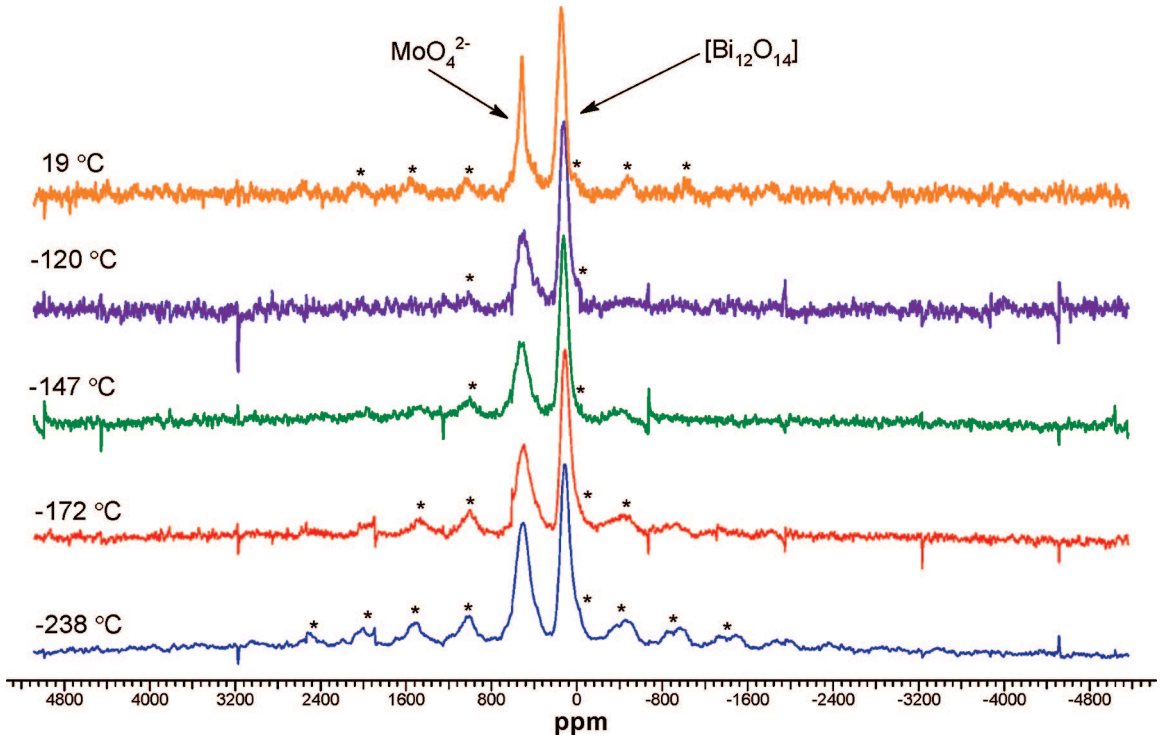

Figure 3. Variable low-temperature ^{17}O MAS NMR spin−echo spectra of $Bi_{26}Mo_{10}O_{69}$ at a field strength of 48.8 MHz and a MAS frequency of 25 kHz. Sidebands due to the MoO_4^{2-} groups are marked with asterisks. Small spikes in the spectra are most likely due to the instability of the low-temperature spinning and the use of He as a spinning gas.

Bi_2WO_6[9]/Bi_2MoO_6, where a shift of 242 ppm was observed for the oxygen ions in the $Bi_2O_2^{2+}$ layers. The resonance is broad due to two effects, (a) the presence of six different O sites within the $[Bi_{12}O_{14}]_\infty$ columns, and (b) line broadening due to residual dipolar coupling to the nearby quadrupolar, $I = 9/2$ ^{209}Bi nuclei,[15] which are associated with extremely large quadrupole moments. The isotropic resonance at 570 ppm is assigned to oxygens in the MoO_4^{2-} units based on work by Emery et al.[16] on $La_2Mo_2O_9$ (= 346−602 ppm for MoO_4 groups), and in WO_4^{2-} units in ZrW_2O_8 (= 434, 561, and 734 ppm).[17] The 570 ppm resonance is comprised of a sharper peak and a broader component in the baseline, the broader component presumably reflecting the distribution of local environments that arise from the three different crystallographically distinct MoO_4^{2-} groups (and hence 12 O sites) that contribute to this resonance. No significant change in the line width (in units of ppm) of the 570 ppm resonance was observed when the spectrum was acquired at a lower field strength (11.7 vs 8.45 T), confirming that the line width is dominated by a distribution of chemical shifts, rather then second-order quadrupolar interactions.

Broad sidebands are seen for the 200 ppm resonance which spread over more than 6000 ppm; these are attributed to satellite transitions from this resonance. In contrast, the much sharper sidebands seen for the 570 ppm resonance, which spread over 1800 ppm (Figure 2), are assigned to sidebands from both the central and satellite transitions of the MoO_4^{2-} ions. According to the structural model proposed by Vannier et al., the interstitial oxygen atom in the O[19] site is coordinated to one Bi^{3+} ion, and weakly coordinated to three MoO_4^{2-} units, and thus, is expected to resonate at a frequency intermediate between the two major groups of resonances. However, this site is only 25% occupied, and will therefore only account for only approximately 1.5% of the intensity. It is presumably too weak to be observed in these spectra, and/or is hidden under the spinning sidebands.

On decreasing the temperature, no significant change in the line width of the $[Bi_{12}O_{14}]_\infty$ resonance is observed (Figure 3). In contrast, the sharp component of the MoO_4^{2-} resonance broadens, and a single broad (asymmetric) resonance is observed at −120 °C, indicative of a distribution of local environments. The line width of the isotropic resonances in a 1D NMR spectrum will be strongly affected if motion is present of the order of the frequency difference between the various resonances. When the hopping frequency of the O^{2-} anions between different sites approaches one-half of this frequency difference, peak broadening is observed. With increasing exchange rates, the peaks broaden further and then coalesce producing a narrow resonance with a shift intermediate between those of the original resonances.[18] Thus, at room temperature, motional processes on the order of the low temperature line width of this resonance (2.12 kHz), involving at least a subset of the MoO_4^{2-} oxygen atoms, must be present resulting in line-narrowing. More obvious, however, is the disappearance and reappearance of

(15) Olivieri, A. C. *Solid State Nucl. Magn. Reson.* **1992**, *1*, 345.
(16) Emery, J.; Massiot, D.; Lacorre, P.; Laligant, Y.; Conder, K. *Magn. Reson. Chem.* **2005**, *43*, 366.
(17) Hampson, M. R.; Evans, J. S. O.; Hodgkinson, P. *J. Am. Chem. Soc.* **2005**, *127*, 15175.
(18) Levitt, M. H. *Spin Dynamics: Basics of Nuclear Magnetic Resonance*; 1st ed.; John Wiley & Sons: New York, 2002.

spinning sideband manifolds arising from the satellite transitions with decreasing temperature.

In a MAS NMR experiment, slow reorientational motion during the rotor period alters the evolution of the spin packets so that they no longer necessarily contribute to echo formation at the end of the rotor period in the free induction decay (FID) and in turn to the formation of spinning sidebands in the spectrum.[19] The time scale of this process is governed by the size of the anisotropic part of the interaction that broadens the resonance (for ^{17}O resonances, this is largely dominated by the quadrupole interaction and to a much lesser extent the dipolar and chemical shift anisotropies (CSA)) and the MAS frequency. Very slow motion of the ions on the order of the spinning frequency will cause a decrease in the intensity and eventually the disappearance of the spinning sidebands. Assuming random isotropic motion, the line broadening due to this mechanism, given by $1/T_2^*$, can be calculated from the following equation[19]

$$T_2^* = 16(\omega_r/\delta\omega_0)^2\tau_c \qquad (1)$$

where $\delta\omega_0$ is the total (static) line width of the resonance or transition (in angular frequency). The line widths can be readily calculated from expressions for the first-order quadrupolar interaction and for the inner and outer satellite transitions of an $I = 5/2$ nucleus and are given by $Q_{cc}(9/80)$ and $Q_{cc}(9/40)$, respectively, where Q_{cc} is the quadrupole coupling constant $= e^2qQ/\hbar$. Unfortunately, the stability of the spinning speed at this temperature was not sufficient to allow spectra with well-resolved satellite transitions to be acquired because the spinning speed instabilities tend to wash out the outer satellite peaks. Furthermore, there is considerable overlap between the satellite transitions of the Bi−O and Mo−O resonances at the spinning speed used at low temperatures (25 kHz). In addition, the width of the satellite transitions may be larger than the bandwidth of the probe. Thus it was not possible to extract an accurate value for Q_{cc}, directly from the low temperature ^{17}O MAS NMR spectra. On the basis of the line width of the observable sideband manifold of approximately 8000 ppm (0.39 MHz) an estimate for the Q_{cc} of 1.6 MHz is obtained (assuming $\eta = 0$), which will represent a lower limit. This value is consistent with typical ranges for the ^{17}O Q_{cc} of 0.5−2.0 MHz, for ions in these types of environments,[9,17,20] but is larger than the Q_{cc} of 0.5 MHz observed for the WO_4^{2-} groups of ZrW_2O_8.[21] This Q_{cc} value was then used to estimate a value for the motional time scale required to prevent refocusing of the rotor echoes and thus for the progressive loss of the satellite transitions above −202 °C. Assuming that the sidebands start to disappear into the baseline when the line-broadening is similar to the spinning frequency, jump frequencies of approximately 1.9 kHz are required for the disappearance of the outer satellites (at approximately −172 °C) and 7.7 kHz for the disappearance of the inner satellites (at approximately −147 °C) (Figure 3). A much smaller set of sidebands is seen at room temperature, indicating that motion

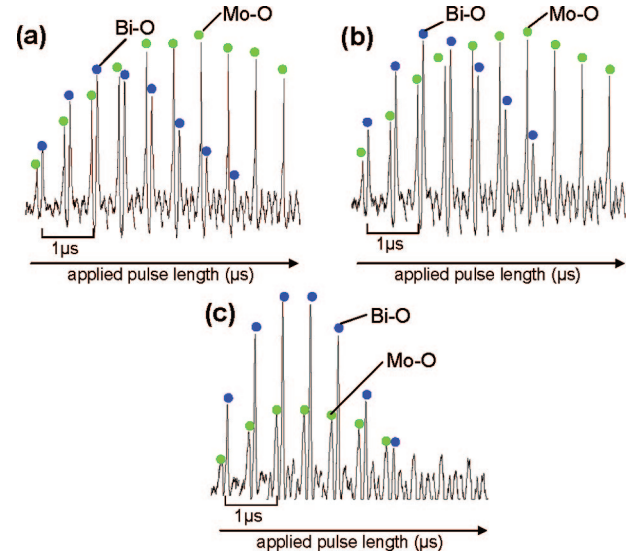

Figure 4. ^{17}O NMR nutation curves for oxygens bonded to bismuth atoms (blue circles) and molybdenum atoms (green circles) in $Bi_{26}Mo_{10}O_{69}$at (a) −40, (b) −70, and (c) −150 °C. Spectra are plotted as a function of the pulse length. The pulse length was incremented in steps of 0.5 μs from 0.5 to 5.0 μs.

on a time scale that is larger than the Q_{cc} of the rigid Mo−O oxygen ions, has resulted in partial averaging of the electric field gradient (EFG) and thus the observation of a reduced Q_{cc}. Only at −238 °C does even the slowest ionic motion cease to affect the refocusing of the rotor echoes.

Nutation Spectroscopy. For quadrupolar nuclei such as ^{17}O, the frequency at which the spins nutate about an applied radio frequency (rf) field (with field strength ω_1) is strongly dependent on the size of the quadrupole frequency (ω_Q) (where ω_Q is given by $(3/20)Q_{cc}$ for a $I = 5/2$ nucleus).[22] For quadrupolar spins in local environments where $\omega_Q < \omega_1$ (i.e., liquid samples or in solids having environments with inherently small quadrupolar couplings, or ones where rapid reorientational motion averages out the quadrupolar interaction), all the $2I$ transitions can be efficiently excited. The nutation frequency is then identical to that observed in the spin-1/2 system and is given by ω_1. For (rigid) local environments associated with large quadrupole coupling constants (Q_{cc}), where $\omega_Q \gg \omega_1$, only the central transition ($|+1/2> - |-1/2>$) of a noninteger spin nucleus is efficiently excited. This partial excitation of the spin system leads to a nutation curve which has $(I + 1/2)$ (i.e., three for ^{17}O) times the frequency but only $1/(I + 1/2)$ times (i.e., one-third for ^{17}O) the amplitude as compared to the above case where all transitions are excited. In this large quadrupole frequency regime, the rf pulse necessary to excite the spin system such that the magnetization is tipped by 90°, is three times shorter than the $\pi/2$ pulse measured for a liquid (e.g., $H_2{}^{17}O$).

The nutation frequency for oxygens associated with bismuth sites in $Bi_{26}Mo_{10}O_{69}$ is approximately three times that of the liquid reference for all temperatures indicating that $\omega_Q \gg \omega_1$ for this site (Figure 4). From this it can be inferred that no ionic motion occurs on the order of the nutation frequency (50 kHz) to result in averaging of the

(19) Maricq, M. M.; Waugh, J. S. *J. Chem. Phys.* **1979**, *70*, 3300.
(20) Adler, S. B.; Reimer, J. A.; Baltisberger, J.; Werner, U. *J. Am. Chem. Soc.* **1994**, *116*, 675.
(21) Hampson, M. R.; Hodgkinson, P.; Evans, J. S. O.; Harrisa, R. K.; Kinga, I. J.; Allena, S.; Fayon, F. *Chem. Commun* **2004**, *2004*, 392.
(22) Vega, A. J. In *Encyclopedia of Nuclear Magnetic Resonance*; Wiley: New York, 1996.

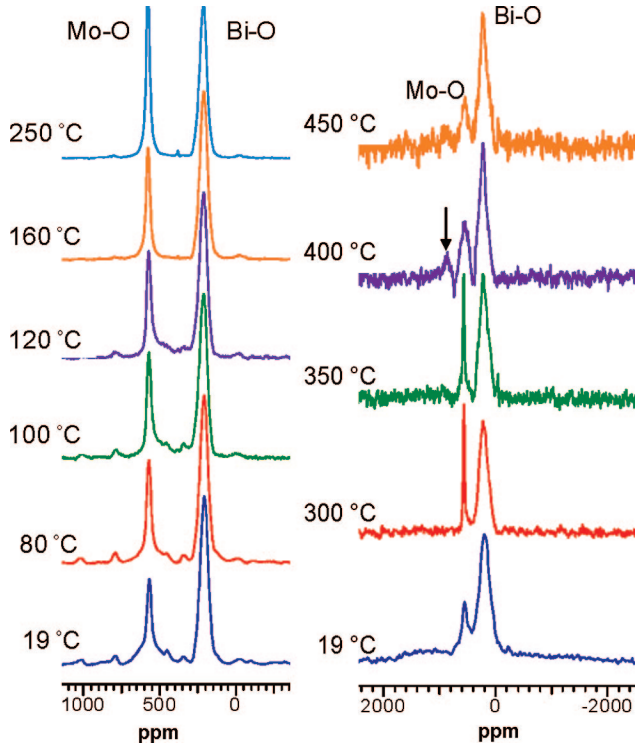

Figure 5. High-temperature ^{17}O NMR spectra of $Bi_{26}Mo_{10}O_{69}$ acquired at a Larmor frequency of 48.8 MHz. Left: MAS NMR spectra from room temperature to 200 °C. Right: static spectra to 450 °C. The arrow in the 400 °C spectrum indicates the peak that is tentatively assigned to the $|3/2\rangle - |1/2\rangle$ satellite transition.

quadrupolar interactions for these sites. In contrast, the nutation frequency of the MoO_4^{2-} oxygens is similar to that of the liquid reference, at room temperature (not shown), −40 and −70 °C, indicating that at these temperatures the effective or averaged value of ω_Q (in the time scale of the nutation experiment) is less than ω_1. At −150 °C; however, the nutation rate of this site increases so as to approach that of the rigid Bi−O site, and the Mo−O spin-system approaches the regime where $\omega_Q \gg \omega_1$. Thus, the nutation curves indicate that at −70 °C and above, oxygen reorientational motion must be occurring on a time scale that is much faster than the time scale of the nutation frequency (i.e., ≫50 kHz), so as to result in averaging of the quadrupolar interaction.

High-Temperature NMR. The high-temperature MAS and static ^{17}O NMR spectra presented in Figure 5 show that the Bi−O peak remains relatively unchanged while the broad component of the MoO_4^{2-} resonance in the MAS spectra narrows significantly above room temperature resulting in a single, sharp resonance at 160 °C, which indicates that all the oxygen atoms of the MoO_4^{2-} units are undergoing very rapid motion at high temperatures. Two types of motion should be distinguished, reorientational motion within the tetrahedra and O exchange between the tetrahedra. The former motion will not contribute (directly) to long-range ionic conductivity. The nutation data and spinning sideband data suggest that at least one of these motional processes is occurring extremely rapidly (with a hop frequency >50 kHz, even at −70 °C). At room temperature, however, a broad line width is still observed (in both the static and MAS spectra) with a line width of 2.12 kHz (MAS), indicating that rapid motion involving all 12 crystallographically distinct Mo−O oxygen atoms cannot be occurring at this temperature, and that there must be a distribution of correlation times for Mo−O motion. This is not inconsistent with the nutation curves presented in the previous section, since these are likely to be dominated by the more rapidly rotating ions, as these are associated with sharper resonances. It is difficult to follow the nutation behavior of the broader resonances, given the poorer S/N of the lower temperature spectra. The results strongly suggest that the rapid motion is likely only occurring within the tetrahedra, since this would result in an effective mechanism for reduction of the quadrupolar interaction (this hypothesis will be confirmed by a comparison with long-range measurements of conductivity, discussed in a later section). Given that there are three crystallographically distinct MoO_4^{2-} units in the unit cell, rapid rotational motion within units, but not between units, would in principle result in the observation of three distinct resonances, the chemical shift of each resonance reflecting the average value for the four oxygens in each individual tetrahedral unit. The observation of only a single resonance at 160 °C, which sharpens considerably up to 350 °C, suggests that exchange is also occurring between the units, on a time scale that is larger than the separation between the four resonances, at this temperature. Because we are not able to observe and assign the resonances from the individual tetrahedra it is difficult to extract an accurate value for the correlation time of this slower motion. However, given the line width of the MoO_4^{2-} resonance at low temperatures (2.1 kHz), motion is likely occurring with a rate greater than this frequency, at 1600 °C and above.

Above 350 °C, significant broadening and loss of intensity of the MoO_4^{2-} resonance can be seen. We tentatively ascribe this phenomenon to the onset of another motional process, possibly involving exchange not only with other oxygens in molybdenum environments, but also with those in bismuth environments. However, this broadening could also possibly be due to other dynamic processes such as the collapse of the satellite transition resonances into the central transition resonance due to the onset of isotropic motional processes occurring at a frequency greater than the Q_{cc}. This latter suggestion, however, does not appear to be consistent with the appearance of a small peak at a higher frequency than the Mo−O peak, at 350 °C, which is ascribed to contributions from the inner satellite transitions, involving the $m = |3/2\rangle$ and $|1/2\rangle$ states with its lower frequency counterpart resonance buried underneath the Bi−O peak. These satellite transitions may give rise to the broad resonance visible in the room temperature spectrum, which then disappears at higher temperatures due to motion. Assuming an asymmetry parameter of 0, an estimate for the Q_{cc} of 250 kHz may be obtained from the position of this peak maximum. The reduced but nonzero Q_{cc} seen at this temperature for the rapidly rotating Mo−O groups is ascribed to the electric field gradients still present at the tetrahedral sites in this highly anisotropic solid with its one-dimensional Bi−O columns.

The chemical exchange between the Mo−O and Bi−O sublattices is confirmed by the ultrahigh temperature static

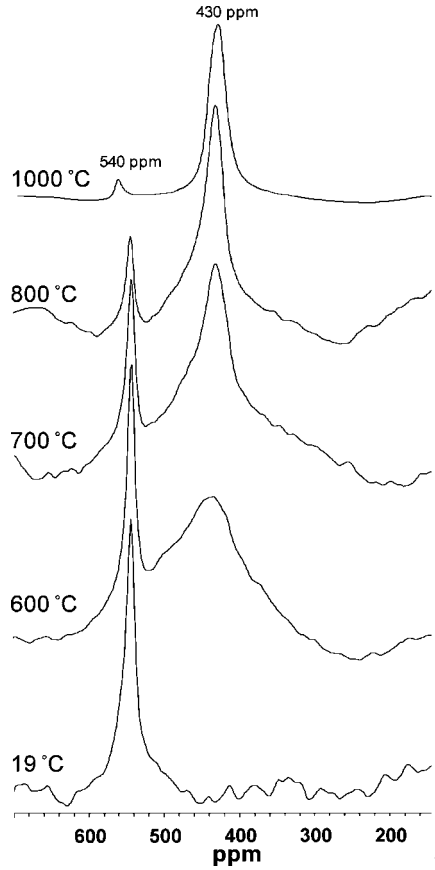

Figure 6. Ultra high temperature, 1 pulse ^{17}O NMR spectra of static $Bi_{26}Mo_{10}O_{69}$, acquired at a field strength of 81.3 MHz.

^{17}O NMR spectra seen in Figure 6. The Bi−O peak, at 200 ppm at room temperature, has completely disappeared, and instead a resonance at a frequency intermediate between that of the Bi−O and Mo−O resonances (430 ppm) is observed at 600 °C. Coalescence occurs when the frequency of hops between the two sites ($1/\tau_c$) is greater or equal to $2^{-1/2}\ \nu_{AB}$, where ν_{AB} is the frequency separation between the two resonances (Mo−O and Bi−O), i.e., $1/\tau_c \geq 55$ kHz for bismuth molybdate at 600 °C. Continued line-narrowing of the 430 ppm resonance occurs as the temperature increases up to 1000 °C, indicating a further increase in the rate of Bi−O, Mo−O exchange.

A weaker resonance due to the MoO_4^{2-} groups is observed, which diminishes in intensity as the temperature is raised. Thus, there is a distribution of correlation times for Bi−O, Mo−O exchange: not all of the MoO_4^{2-} groups are involved in the rapid exchange process, even at these elevated temperatures. This is an important observation, because it indicates that rapid exchange (where rapid is defined as ≫55 kHz) between all the MoO_4^{2-} groups cannot be occurring even at 1000 °C. If rapid exchange between all the MoO_4^{2-} groups was indeed occurring, along with a distribution of correlation times for exchange Bi−O, Mo−O exchange, then all the MoO_4^{2-} oxygen-ion are rendered equivalent in the time scale of the Bi−O, Mo−O exchange. In this case, the MoO_4^{2-} resonance would be expected to shift gradually from its ambient temperature position (540 ppm) to higher frequencies as more and more Bi−O oxygen atoms exchange with the Mo−O oxygen atoms with rates approaching 55 kHz. This phenomenon was observed previously in spectra of LaF_3 and Sr^{2+}-doped LaF_3.[23] Surprisingly, no residual Bi−O peaks remain, indicating that all the Bi−O oxygen atoms, even in the center of the columns, undergo exchange.

Spin−Lattice Relaxation Times. Very fast moving ions on the order of the Larmor frequency (ω_0; typically 10−100 MHz for ^{17}O) will influence the longitudinal (T_1) relaxation time. In principle, ^{17}O relaxation can be driven by two different mechanisms:[24] quadrupolar and/or magnetic. Quadrupolar relaxation, as a general rule does not follow a single exponential decay process, because of the possibility of different transition rates between the different spin-states $|m_I\rangle$[24] (see Yesinowski et al. and Suter et al. for recent discussions of this phenomena[25,26]). The relaxation time of a noninteger spin quadrupolar nucleus will be the sum of I + 1/2 decaying exponential terms,[22,27,28] i.e., for $I = 5/2$ nuclei such as ^{17}O, the relaxation process will involve three exponential terms. However, the relative contribution of the different terms depends on both how the spin system is initially excited and the relative importance of the transition rates W_n involving single (ω_0) and double quantum transitions ($2\omega_0$), W_1 and W_2, respectively. For excitation of the central transition only (i.e., $\omega_Q \gg \omega_1$) and assuming that $W_1/W_2 = 1$ an expression of the form[29]

$$I(t) = I - 0.029\exp(-0.8W_1t) - 0.794\exp(-1.5W_1t) - 0.178\exp(-3.3W_1t) \quad (2)$$

is derived. If the correlation time is short, i.e., when the electric field gradients are fluctuating much more rapidly than the Larmor frequency, however, as occurs in a liquid, the decay expressions will collapse to a single exponential.[27]

In diamagnetic systems, the quadrupolar mechanism generally dominates,[30] because of the much larger sizes of the fluctuating fields caused by the quadrupolar interaction than by for example, the dipolar coupling to nearby mobile ions, or the chemical shift anisotropy. Magnetically driven relaxation occurs primarily when there is a high density of paramagnetic relaxation centers or if the nuclear quadrupole moment is sufficiently small such that the quadrupole relaxation mechanism cannot compete. In their studies of zirconium tungstate, a compound that contains mobile WO_4^{2-} ions, Hodgkinson and Hampson somewhat surprisingly concluded that their ^{17}O T_1 data was better fit to a model based on a magnetic relaxation mechanism, where the relaxation was driven by motion of other ^{17}O nuclei.[17,21] However, given the complexities introduced by multiexponential T_1 relaxation they acknowledged that it would be

(23) Wang, F.; Grey, C. P. *Chem. Mater.* **1997**, *9*, 1068.
(24) Andrew, E. R.; Tunstall, D. P. *Proceedings of the Physical Society* **1961**, *78*, 1.
(25) Suter, A.; Mali, M.; Roos, J.; Brinkmann, D. *J. Magn. Reson.* **2000**, *143*, 266.
(26) Yesinowski, J. P. *J. Magn. Reson.* **2006**, *180*, 147.
(27) Hubbard, P. S. *J. Chem. Phys.* **1970**, *53*, 985.
(28) Bull, T. E.; Forsen, S.; Turner, D. L. *J. Chem. Phys.* **1979**, *70*, 3106.
(29) Gordon, M. I.; Hoch, M. J. R. *J. Phys. C: Solid State Phys.* **1978**, *11*, 783.
(30) Werbelow, L.; Pouzard, G. *J. Phys. Chem.* **1981**, *85*, 3887.
(31) Narayanan, A.; Hartman, J. S.; Bain, A. D. *J. Magn. Reson., Ser. A* **1995**, *112*, 58.

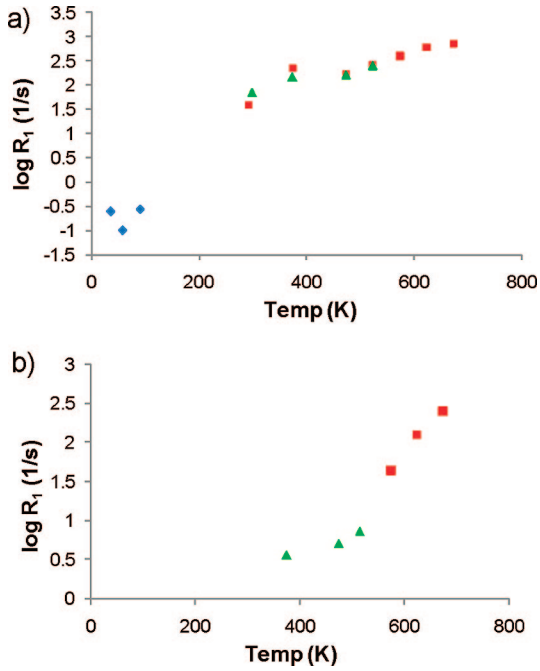

Figure 7. Relaxation rates, R_1 ($1/T_1$) versus temperature for oxygens in (a) molybdenum environments and (b) bismuth environments in $Bi_{26}Mo_{10}O_{69}$. Blue diamonds represent data acquired on the 1.8 mm MAS cryostat probe, green triangles represent data acquired on a 4 mm MAS probe, red squares represent data acquired on a 5 mm static high-temperature probe.

difficult to use ^{17}O NMR to distinguish between these mechanisms as they have such similar overall effects. The analysis of their system was further complicated by the relatively slow exchange that occurs between the different oxygen ions in the WO_4^{2-} ions, so that the overall relaxation was a sum of multiple different rates. Given the complexity involved in interpreting relaxation data, several groups have used a stretched exponential function to describe a distribution of relaxation times[31]

$$M(\infty)=M(t)(1-\exp[-(t/T_1)^{\beta}]) \quad (3)$$

where β is the stretch exponent with $0 < \beta \leq 1$. Although lacking the physical significance of some of the more sophisticated fittings, this method does represent a convenient and practical model for characterizing nonexponential relaxation in solids. It is also a reasonable approximation because, even in models that consider more than one rate, the relaxation process is generally dominated by a single rate (i.e., $1.5W_1$ in eq 2). Thus, we have chosen to use this approach in this work.

T_1 relaxation rates ($1/T_1$) were calculated by using eq 3 and are plotted as a function of temperature for the oxygens in the two environments of $Bi_{26}Mo_{10}O_{69}$ in Figure 7. Stretched exponents, β, of close to 0.5 were required to fit the T_1 data, reflecting both the large numbers of crystallographic sites (presumably each with slightly different correlation times for motion and different Q_{cc}s), and the complex nature of the ^{17}O relaxation processes. Both oxygen environments are associated with relaxation rates that increase with temperature, gradually at low temperatures and then much more rapidly above 310 °C, the triclinic-to-monoclinic phase transition temperature. However, there is a far more profound discontinuity in the relaxation rates for oxygens in bismuth environments than for those in molybdenum environments at this phase transition temperature. The rapid relaxation times for the Bi−O ions at high temperatures are surprising as both the static and MAS spectra are not consistent with motion for these ions on the Larmor frequency time scale. Two mechanisms can be envisaged that will result in rapid T_1 relaxation. First, the Bi−O oxygen atoms, although not mobile themselves, will nonetheless experience fluctuations in the electric field gradients, due to rapid motion of nearby charged ions. This mechanism was previously proposed to explain the short T_1 times seen for $[Bi_2O_2]^{2+}$ O ions in doped Bi_2WO_6 in temperature regimes where they are not themselves mobile[9] and for the rigid oxygen-sublattices of Zr-doped $Ba_2In_2O_5$.[32] A second mechanism involves the exchange between the Bi−O and Mo−O ions, the T_1 relaxation rate representing a measure of the exchange rate between the two sublattices. This mechanism was shown to be responsible for the short relaxation times of F^- ions in the "rigid" BaF_2 sublattice of $BaSnF_4$.[33] Undoubtedly, the first mechanism will contribute in part to the gradual decrease in the T_1 time with temperature, and the decrease should track the decrease in the Mo−O relaxation times directly. The discontinuity in the Bi−O relaxation rates (but not in the Mo−O rates) at the phase transition cannot, however, be ascribed to this mechanism, and it strongly suggests that exchange between the Bi−O and Mo−O sublattices must also be occurring. This observation is consistent with the line shape changes of the Mo−O resonances seen in Figure 5 in this temperature regime and the coalescence seen for the Mo−O and Bi−O resonances at higher temperatures.

Discussion

Interpretation of the T_1 Data; Implications for Local and Long-Range Motion. The relaxation data can be used to extract a correlation time, τ_c (τ_c = 1/ hop frequency) for the motion that drives the increase in relaxation, via equations of the form[34]

$$\frac{1}{T_1}=\frac{3}{625}Q_{cc}{}^2\left(1+\frac{\eta^2}{3}\right)\left[\frac{a\tau_c}{1+\omega_0{}^2\tau_c{}^2}+\frac{4b\tau_c}{1+4\omega_0{}^2\tau_c{}^2}\right] \quad (4)$$

This equation is specific to a spin 5/2 system and assumes that the major driving force for relaxation comes from the quadrupole interaction, quantified via Q_{cc} and the asymmetry parameter, η. The numerical coefficients a and b reflect the geometric details of the motion, and the multiexponential character of the decay (e.g., the W_1/W_2 ratio, the state of the initial spin system etc.). $a = b = 1$ in the case of rapid fluctuations of the EFG tensor; this is assumed in this work, which although an approximation, allows approximate orders of magnitude for $\tau_c$to be extracted.

(32) Adler, S.; Russek, S.; Reimer, J.; Fendorf, M.; Stacy, A.; Huang, Q.; Santoro, A.; Lynn, J.; Baltisberger, J.; Werner, U. *Solid State Ionics* **1994**, *68*, 193.
(33) Chaudhuri, S.; Wang, F.; Grey, C. P. *J. Am. Chem. Soc.* **2002**, *124*, 11746.
(34) Speiss, H. W. In *NMR−Basic Principles and Progress*; Diehl, P.; Fluck, E.; Kosfeld, R.; Springer-Verlag: Berlin, 1978; Vol. 15, p 117.

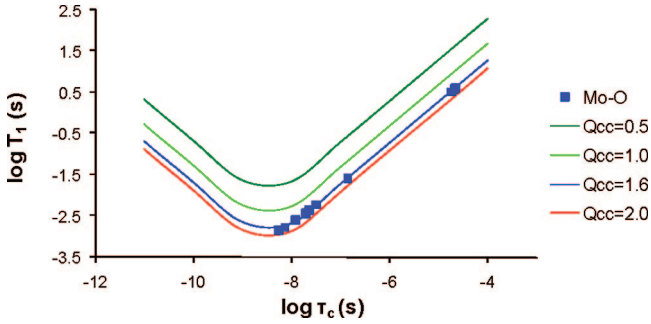

Figure 8. ^{17}O NMR T_1 relaxation time for oxygen nuclei in molybdenum environments in $Bi_{26}Mo_{10}O_{69}$ at 8.5 T vs calculated correlation times with a quadrupole coupling constant of 1.6 MHz. General T_1 vs τ_c curves for a 5/2 system at a field of 8.5 T, from top to bottom calculated with Q_{cc} = 0.5, 1.0, 1.6, and 2.0 MHz, respectively. The blue squares represent the experimental data in the temperature range from 35 to 673 K.

The T_1 relaxation times for the molybdenum oxygen environment are plotted versus correlation time, calculated from eq 4 in Figure 8. A quadrupole coupling constant of 1.6 MHz was assumed, which represents the estimate for the Q_{cc} made on the basis of the low-temperature MAS data, and then fitted to the calculated general curve for a 5/2 system at this field. As demonstrated via calculating general T_1/τ_c curves for other Q_{cc}′s, as shown in this figure, Q_{cc} values of smaller than 1.6 MHz do not result in a sufficiently large reduction in the τ_c. Thus, this Q_{cc} value also represents the minimum possible value for the Q_{cc} required to produces the experimentally observed decreases in the T_1 time for the Mo−O sites, assuming that the quadrupolar relaxation mechanism represents the dominant relaxation mechanism. Because no clear T_1 minimum is observed in the data, we cannot exclude the possibility that the Q_{cc} is actually slightly larger. As illustrated in Figure 8, an increase in the Q_{cc} from 1.6 to 2.0 MHz, results in a change in calculated correlation time, τ_c by approximately 55%. The Q_{cc} cannot be significantly larger than 2.0 MHz, because we did not observe any evidence for broadening of the isotropic (central transition) resonance, due to the second order quadrupolar interaction, even at the lower magnetic field strengths. The hop frequencies extracted from these T_1 measurements are surprisingly large, varying from 12 kHz at −238 °C, ∼5 MHz at room temperature, and 78 MHz at 400 °C. These values are consistent with the hop frequencies estimated based on the analyses of the nutation curves and the line widths of the spinning sidebands at lower temperatures. Furthermore, the higher temperature values are consistent with the averaging of the first order quadrupolar interaction and the reduction of the Q_{cc} from approximately 1.6 MHz to 250 kHz, indicating that motion on the MHz time scale is occurring at these temperatures. Errors in our assumption concerning the two constants, a and b, in eq 4 do not affect these general conclusions. If we assume that $b = 0$, no noticeable change in the calculated hop frequency is observed. The Bi−O hop frequencies were similarly calculated by assuming a Q_{cc} for this site of 1.6 MHz, this value for the Q_{cc}, (as for the Mo−O sites) representing the minimum size of the Q_{cc} fluctuation required to produce the experimentally observed T_1 values.

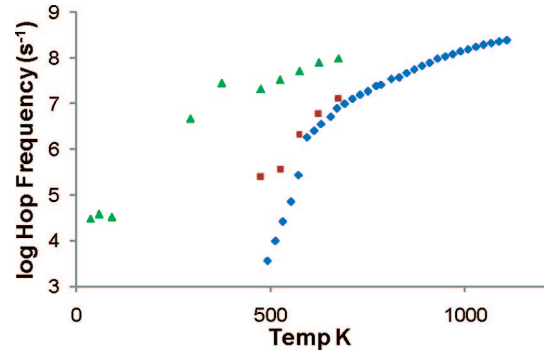

Figure 9. Comparison of oxygen hop frequencies versus temperature calculated from conductivity data[2] (blue diamonds) with those calculated from NMR T_1 data for Bi−Os site (red squares) and Mo−O sites (green triangles).

Comparison between Long- And Short-Range Motion. We now compare the hop frequencies for oxygens at various temperatures determined by NMR, with those calculated from conductivity measurements in order to determine if the motion causing the effects in the NMR experiments is due to long-range or local movement of the ions. The hop frequencies for motion that contribute to long-range conductivity can be calculated from conductivity measurements using the Nernst−Einstein equation

$$\sigma \frac{k_B T}{Nq^2} H_R = D^T \tag{5}$$

And the Einstein−Smoluchowski relationship

$$\tau_c^{-1} \frac{r^2}{6} f = D^T \tag{6}$$

where σ is the conductivity, H_R is the Haven ratio, q is the charge, T is the temperature, N is the number of charge carriers, k_B is the Boltzmann constant, D^T is the tracer diffusivity, f is the correlation factor, and τ_c^{-1} is the hop frequency. The hop frequencies obtained from these equations and previous conductivity measurements for this system[4] are compared with those obtained from the T_1 relaxation data in Figure 9. We assumed a Haven ratio and correlation factor of 1, a jump distance of 3 Å, representing the average distance between MoO_4^{2-} units, that O^{2-} is the only charge carrier contributing to conductivity. Although these assumptions may not be justified at all temperatures, the jump rates calculated from the conductivity measurements are less than those calculated from the NMR relaxation data of the Mo−O site by several orders of magnitude, a conclusion that is not affected by these assumptions. This result indicates that the very rapid oxygen motion of the Mo−O tetrahedra causing the NMR relaxation is most likely localized and does not contribute to long-range conductive hopping at low-intermediate temperatures. The jump rates of the O ions on the Bi−O sites, as measured by the NMR relaxation data do, however, approach those calculated from conductivity data at higher temperatures, strongly implying that the two methods do in fact examine the same motional processes. This is provides further support for our proposal that the high temperature, long-range conductive process in this material involves exchange between oxygens ions bonded to the molybdenum and those bonded to bismuth ions.

Conclusions: Implications for Motion in $Bi_{26}Mo_{10}O_{69}$

The rates of oxygen motion for two major types of oxygen environments in $Bi_{26}Mo_{10}O_{69}$ have been determined by a wide variety of ^{17}O NMR methods, over an extremely large range of temperatures. Nutation studies, analysis of the changes in line widths of the satellite transitions and T_1 relaxation data, all consistently indicate that very rapid motion, with associated jump frequencies on the order of 1×10^4 to 1×10^5 Hz commences even at very low temperatures. For example, analysis of the sideband manifolds indicates that hop frequencies greater than 2 kHz at −172 °C, and 7 kHz at −147 °C are occurring. This motion becomes extremely rapid above room temperature, the relaxation data indicating that motion of the order of 30 MHz occurs at 100 °C; the observation of a reduction in the Q_{cc} on the time scale of the quadrupolar interaction at 300 °C also suggests that motion on the MHz time scale is occurring. Despite this evidence for extremely rapid motion, coalescence of the broad and narrower components of the MoO_4^{2-} isotropic resonance only occurs above 160 °C, indicating that not all of the oxygen ions in the MoO_4^{2-} groups undergo rapid chemical exchange with each other (i.e., rapid inter-tetrahedral exchange is not occurring between all the ions). Furthermore, long-range (ac conductivity) measurements in this temperature regime are consistent with hop rates between MoO_4^{2-} ions that are almost 4 orders of magnitude less than the hop rates extracted for these ions from the relaxation data (e.g., a hop rate between O sites of only 3.5 kHz is calculated at 200 °C from the ac conductivity data (Figure 9)). We therefore, ascribe the more rapid motion to the rotation of the individual MoO_4^{2-} tetrahedra. This is consistent with the large thermal parameters seen for the Mo−O oxygen atoms in the structural refinements[2] and indicates that the thermal parameters do not necessarily provide a good measure of the sublattice and mechanism responsible for long-range anionic conductivity. This extremely rapid MoO_4^{2-} rotation is most likely assisted by the presence of lone pairs on the Bi^{3+} ions, which point directly toward the MoO_4^{2-} tetrahedra. This motion does not directly give rise to long-range conductivity. Long-range anionic conductivity in this temperature range is ascribed to slow exchange between the MoO_4^{2-} tetrahedra (on the order of >2 kHz at this temperature). The mechanism by which this occurs is discussed below.

At 350 °C, above the phase transition, exchange occurs between the Mo−O and Bi−O sublattices, as indicated by the increase in the Mo−O line width, the noticeable increase in the Bi−O T_1 relaxation rate, and the coalescence of the Bi−O and MoO_4^{2-} resonances at 600 °C. No Bi−O resonances remain, indicating that oxygen exchange between the ions in the center and outer shell of the $[Bi_{12}O_{14}]_\infty$ columns occurs. These columns adopt the fluorite structure, which is also the structure of the high temperature form of Bi_2O_3, δ-Bi_2O_3, which similarly exhibits high oxide ion conduction.[35] Once an oxygen vacancy is introduced into the Bi−O lattice, the proposal that oxygen diffusion occurs appears to be quite reasonable.[36–42] In this temperature regime, the hop frequencies of the Bi−O oxygen atoms and those calculated from the ac impedance measurements approach each other. Taken together, these observations strongly suggest that the long-range conductive processes now start to involve the Bi−O sites, even in the $[Bi_{12}O_{14}]_\infty$ columns. However, there is no evidence for rapid exchange within the $[Bi_{12}O_{14}]_\infty$ columns before the onset of the Bi−O and Mo−O exchange indicating that long-range conductivity cannot be ascribed to motion only involving the $[Bi_{12}O_{14}]_\infty$ columns. Finally, both a jump in the long-range conductivity (by almost an order of magnitude) and a decrease in the activation energy are seen at the phase transition temperature,[3] also suggesting that different conductivity mechanisms are operating above and below the phase transition temperature, with an increasing number of charge carriers at elevated temperatures.

Long-range motion involving only the MoO_4^{2-} ions is expected to be extremely slow, because it requires the concerted creation of both lower and higher coordinate $MoO_n^{(6-2n)-}$ ions as presumably short-lived defects or intermediate states. The low-coordinate environment, in particular, is likely to be associated with a very high energy of formation resulting in a high activation energy for this processes. Vannier et al. have suggested that the long-range conductive mechanism for bismuth molybdate involves the vacancies at the isolated, but partially occupied, Bi−O O[19] sites.[4] The O[19] site is in close proximity to Mo(3) and Mo(1) oxygen atoms, and is also strongly bonded to Bi(4) and Bi(5) (Figure 1a) with calculated Bi(4)−O[19] and Bi(5)−O[19] bond lengths of 1.97(7) Å and 2.56(3)Å, respectively. These vacant O[19] sites can provide a source of additional oxygen ions/vacancies, so that the conduction mechanism no longer requires the albeit transient formation of low coordinate $MoO_n^{(6-2n)-}$ ions. This allows a motional process with a lower activation energy to proceed involving the transfer of an O[19] to a nearby vacant O[19] site via an intervening MoO_4^{2-} ion (Figure 10). This process is mediated via the extremely rapid rotation of the MoO_4^{2-} ions. Since the closest O[19] sites are along the b- (the column) direction and are 6 Å apart, and only separated by one intervening $Mo(3)O_4^{2-}$ or $Mo(1)O_4^{2-}$ tetrahedral unit, as shown schematically in Figure 10, conduction along the *b*-direction, as proposed by Vannier et al., appears reasonable. Motion in the *a*−*c* plane will occur much less frequently, because it involves a jump-process with concerted bond breakages of Mo−O bonds in multiple tetrahedra. For example, O[19] sites are separated by over 9 and 11 Å and two and 4 MoO_4^{2-} tetrahedra in the *c*- and *a*-directions, respectively. Given the low occupancy of the proposed O[19] site, however, it is difficult to determine by NMR the role

(35) Wachsman, E. D.; Boyapati, S.; Kaufman, M. J.; Jiang, N. *Proceedings of the Symposium on Solid State Ionic Devices*, Seattle, May 2−7, 1999; The Electrochemical Society: Pennington, NJ, 1999; *99−13*, 42.
(36) Yaremchenko, A. A.; Kharton, V. V.; Naumovich, E. N.; Tonoyan, A. A. *Mater. Res. Bull.* **2000**, 35.
(37) Medvedeva, N. I.; Zhukov, V. P.; Gubanov, V. A.; Novikov, D. L.; Klein, B. M. *J. Phys. Chem. Solids* **1996**, 57.
(38) Subbarao, E. C.; Maiti, H. S. *Solid State Ionics* **1984**, *11*, 317.
(39) Takahashi, T.; Iwahara, H.; Nagai, Y. *J. Appl. Electrochem.* **1972**, 2.
(40) Takahashi, T.; Iwahara, H.; Esaka, T. *J. Electrochem. Soc.* **1977**, 124.
(41) Takahashi, T.; Iwahara, H. *J. Appl. Electrochem.* **1973**, 3.
(42) Hapase, M. G.; Tare, V. B.; Biswas, A. B. *Indian J. Pure Appl. Phys.* **1967**, *5*, 401.

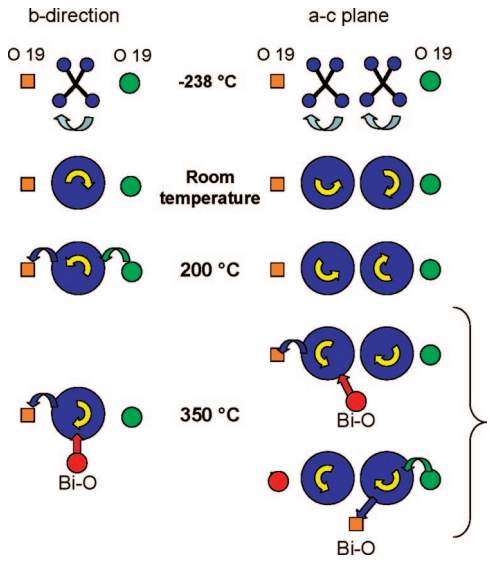

Figure 10. Schematic illustrating the dominant motions in $Bi_{26}Mo_{10}O_{69}$ at different temperatures. At low temperatures, rotational motion of the MoO_4^{2-} ions commences, as illustrated by the light green arrow. By room temperature, this motion is so rapid on the scale of any long-range motion, that the tetrahedra may be viewed as rapidly rotating balls on this time scale. By 200 °C, concerted motion involving filled and empty O[19] sites and the MoO_4 tetrahedra has commenced. Above the phase transition, additional motion involving oxygen atoms from the Bi−O columns begins; this motion can occur in both the *b* and *a*−*c* directions and does not require concerted Mo−O bond breakage in more than one MoO_4^{2-} tetrahedral unit.

that this site, or another low occupancy interstitial site in the structure, plays in the process at ambient temperatures. However, the current NMR data clearly indicate that the motion below the phase transition primarily involves motion between the MoO_4^{2-} ions.

Above the phase transition, the NMR data indicates that there is an additional mechanism of motion which now involves more of the Bi−O oxygen atoms. These oxygen atoms now appear to serve as possible sites for vacancies (Figure 10) and motion is now permitted in three dimensions. No oxygen vacancy was identified on these column sites in the structural refinements[4,7] performed at room temperature. However, as the temperature is increased, the energy associated with vacancy formation on the Bi−O column will decrease relative to *kT* (the thermal energy) and formation of oxygen vacancies appears to be possible. The O−O distances obtained at room temperature[4] between O[5] and O[17], O[5] belonging to the column and O[17] to the nearby $Mo(3)O_4^{2-}$ tetrahedron (see Figure 1), is 2.82, whereas the O[17] to O[19] distance is only 2.52 Å. Therefore, a hop of the O[19] vacancy to an O[17] site, as described above, can readily occur. Further migration of this vacancy to the nearby O[5] site is then possible, which will result in a three-dimensional diffusion process involving both the Bi−O and Mo−O sublattices. The observation of residual MoO_4^{2-} groups at very high temperatures indicates that not all the MoO_4^{2-} groups are involved in rapid exchange. This suggests that while at these temperatures, rapid motion occurs in the *a*−*c* plane, as proposed by Galy et al.,[5] exchange involving all the tetrahedra is not occurring.

The motion observed in this system is quite different to that seen by Hampson et al. for ZrW_2O_8.[17] They were able to resolve the individual oxygen sites within the tungstate tetrahedra and observed exchange between all the O sites at close to ambient temperatures. Although this motion involves two adjacent WO_4^{2-} tetrahedra, (the $W_2O_8^{4-}$ units), again the exchange in this temperature regime involves motion only within the individual tetrahedra, and not between the anions. They proposed a local, reorientational or "ratcheting"-type motion of the $W_2O_8^{4-}$ units, based on the exchange rates between the different types of oxygen atoms, which could account for the negative thermal expansion seen for this material. The reorientational motion seen here in $Bi_{26}Mo_{10}O_{69}$is 2 orders of magnitude faster, which is ascribed to the presence of the large, highly polarizable Bi^{3+} ions with their stereoactive lone pairs.

In conclusion, this work has demonstrated that it is possible to unravel the mechanisms that contribute to both short and long-range conductivity in an extremely structurally and dynamically complex material $Bi_{26}Mo_{10}O_{69}$, by using both short- (NMR) and long-range (ac impedance) probes of motion. The NMR analysis required that a large number of different ^{17}O NMR experiments were performed over a wide range of temperatures. We demonstrate that rotational motion of the MoO_4^{2-} units is extremely rapid even at very low temperatures, consistent with the large thermal parameters seen for the O sites of these units[4]. The results indicate that care must be taken when using large thermal parameters as an indication of long-range motion. A new mechanism is proposed to explain the high temperature conductivity of this material that involves oxygen atoms in both the MoO_4^{2-} and Bi−O sublattices. The mechanism involves O^{2-} hops between oxygen sites coordinated to Bi^{3+} ions, involving intermediate MoO_4^{2-} tetrahedra. The tetrahedra undergo very rapid reorientations, mediating the transport process indirectly: i.e., the rate limiting process for conduction will be associated with Mo−O bond breakage, rather than MoO_4^{2-} reorientation, since the latter process is extremely rapid on the time scale of the Mo−O bond breaking process. Although conduction is likely occurring in all three directions, the proposal by Vannier et al. that conduction in the b-direction is more rapid than in the *a*−*c* plane appears reasonable for 2 reasons, (i) conduction in this direction can occur in the absence of Mo−O, Bi−O column exchange, (via the O[19] sites), without involving concerted Mo−O bond breakage on multiple MoO_4^{2-} tetrahedra and (ii) resonances due to isolated MoO_4^{2-} ions (i.e., O^{2-} in tetrahedra not undergoing rapid exchange with Bi−O ions or between tetrahedra), are seen at very high temperatures, suggesting that rapid motion involving all the tetrahedra equally is not occurring.

Acknowledgment. This work was supported in part by Grant DMR050612 from the National Science Foundation and Grant DEFG0296ER14681 from the Department of Energy. We also thank Ago Samoson for his invitation to perform ultra low temperature experiments, the International Center for Materials Research at UC Santa Barbara for travel funding (NSF Grant DMR 0409484), and Dr. Sylvio Indris for helpful discussions. I.H. thanks the Estonian Science Foundation for support by Grant 6846 and M.E.S. thanks the EPSRC and the University of Warwick for partial funding of NMR equipment at Warwick.

CM800351C